Discriminating between Higgs Production Mechanisms via Jet Charge at the LHC

Hai Tao Li,[1,*] Bin Yan,[2,†] and C.-P. Yuan[3,‡]
[1]School of Physics, Shandong University, Jinan, Shandong 250100, China
[2]Institute of High Energy Physics, Chinese Academy of Sciences, Beijing 100049, China
[3]Department of Physics and Astronomy, Michigan State University, East Lansing, Michigan 48824, USA

(Received 28 January 2023; revised 28 April 2023; accepted 10 July 2023; published 24 July 2023)

Discriminating between Higgs production mechanisms can play a crucial role in determining the couplings of Higgs to gauge bosons, probing the nature of electroweak symmetry breaking. We propose a novel method to distinguish the Higgs production mechanisms at the LHC by utilizing the jet charge asymmetry of the two leading forward jets in Higgs plus two jets production. This novel observable provides a way to disentangle the W fusion from the Z fusion and gluon fusion processes for the first time, due to the electric charge correlation of the two leading jets in the events. We show that the Higgs couplings to gauge bosons can be well constrained, and its conclusion does not depend on the other possible new physics effects which modify the Higgs total or partial width. We also discuss the complementary roles between the proposed jet charge asymmetry measurement and the Higgs signal strength measurements at the high luminosity LHC (HL-LHC) in determining the Higgs couplings.

DOI: 10.1103/PhysRevLett.131.041802

Introduction.—Precisely measuring the interactions between the Higgs boson and the weak gauge bosons (W and Z) can play a crucial role to verify the electroweak symmetry breaking (EWSB) mechanism of the Standard Model (SM) and beyond. These couplings have been widely discussed under the framework of the κ scheme or the Standard Model effective field theory (SMEFT) at the Large Hadron Collider (LHC) and future colliders [1–18]. From the recent global analysis of the ATLAS [19] and CMS [20] Collaborations at the 13 TeV LHC, the magnitudes of these couplings have been severely constrained by the Higgs data within an uncertainty of about $\mathcal{O}(10\%)$, i.e. $\kappa_W = 1.05 \pm 0.06$, $\kappa_Z = 0.99 \pm 0.06$ (ATLAS) and $\kappa_W = 1.02 \pm 0.08$, $\kappa_Z = 1.04 \pm 0.07$ (CMS), where $\kappa_{W,Z}$ are the effective gauge coupling strengths between the Higgs boson and the W and Z bosons, respectively:

$$\mathcal{L}_{hVV} = \kappa_W g^{\mathrm{SM}}_{hWW} h W^+_\mu W^{-\mu} + \frac{\kappa_Z}{2} g^{\mathrm{SM}}_{hZZ} h Z_\mu Z^\mu, \qquad (1)$$

where $g^{\mathrm{SM}}_{hVV} = 2m_V^2/v$, with $V = W, Z$, are the Higgs couplings to gauge boson V in the SM, and $v = 246$ GeV is the vacuum expectation value.

However, to date, all the knowledge of the Higgs couplings is inferred from the global analysis of the Higgs data under the narrow width approximation for the Higgs production and decay. As a result, the measurements of the Higgs properties strongly depend on the assumption of the Higgs width, which is difficult to be determined at the LHC [19,20]. Therefore, probing the Higgs couplings with the fewest possible theoretical assumptions (e.g., Higgs width) can play a crucial role to verify the nature of the EWSB. One of the approaches to overcome the shortness of the current global analysis is to measure the off shell Higgs signal strengths [21–24]. Unfortunately, the Higgs cross sections decrease so fast in the off shell Higgs phase space region that it would be a challenge to measure the Higgs couplings with a high accuracy [25,26]. Moreover, generally, the determination of the Higgs couplings also depends on other theoretical assumptions made in the analysis [23,27–32].

For the purpose of determining the hVV couplings, the mechanism of Higgs production via vector boson fusion (VBF) plays an essential role at the LHC. The representative Feynman diagrams at the leading order are shown in Fig. 1. Since the Higgs + 2 jets production through the gluon-gluon fusion (GGF) process is the dominant background for the VBF Higgs production at the LHC, the attempt of separating the VBF from the GGF production

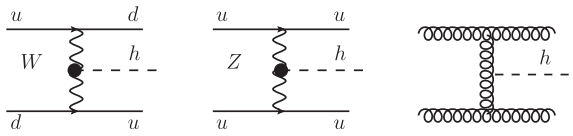

FIG. 1. Illustrative Feynman diagrams of VBF and GGF Higgs + 2 jets production at the LHC. The black dots denote the effective Higgs couplings to gauge bosons.

has been widely discussed [33–41]. It shows that the contribution from the GGF process can be largely suppressed by requiring a large rapidity gap and a large invariant mass of the two hardest jets in the Higgs + 2 jets events [33–35]. We can also utilize the different features of soft gluon radiations between the VBF and GGF processes to suppress the contribution from the GGF, e.g., the difference in the jet energy profiles [36] and the azimuthal angle correlation between the Higgs and two-jet system [37,40]. But, none of them could distinguish WW and ZZ-boson fusion processes. Separating the W boson's contribution from the VBF Higgs production is an important task for determining κ_W and κ_Z, separately, at the LHC.

To suppress the contributions from the Z-boson fusion and the GGF processes, we define a novel observable called *jet charge asymmetry* between the two leading jets in the Higgs + 2 jets production. For the first time, we demonstrate that the jet charge correlations in Higgs + 2 jets production can be used to separate the W-boson fusion from the Z-boson fusion and GGF processes; the electric charges of the two leading jets in W-boson fusion are opposite, while they could be the same or opposite for the Z-boson fusion and the GGF processes. We argue that one could determine the $\kappa_{W,Z}$ without making an assumption on the Higgs width and the other possible new physics effects from Higgs decay. Moreover, the correlation between κ_W and κ_Z, obtained from the jet charges' measurement, would be different from other experimental observables (e.g., the Higgs signal strength measurement) in the VBF processes. Therefore, the jet charge correlation in the production of Higgs + 2 jets could play an important, and complementary, role in determining the hVV couplings.

Jet charge.—Jet charge can be used to mimic the electric charge of the parent parton which evolves into a collimated spray of particles. It is defined as a weighted sum of the electric charge of the jet constituents [42–44],

$$Q_J = \frac{1}{(p_T^J)^\kappa} \sum_{i \in \text{jet}} Q_i (p_T^i)^\kappa, \qquad \kappa > 0, \tag{2}$$

with p_T^J the transverse momentum of the jet, p_T^i and Q_i the transverse momentum and electric charge of particle i inside the jet. And κ is a free parameter which suppresses the contribution from soft radiations. The theoretical framework to calculate jet charge in QCD was proposed in Refs. [43,44]. As one of the jet substructure techniques, jet charge has been used for quark-gluon jet discrimination [45–47]. There are many efforts using jet charge as a tool to tag the hard process [48] and to search for new physics signals [49,50]. Jet charge has also been applied to probe nuclear medium effects in heavy-ion and electron-ion collisions [51–53], as well as quark flavor structure of the nucleon [54–56]. Experimentally, jet charge has been recently measured by ATLAS and CMS Collaborations [57–60]. The theoretical and experimental efforts show that the jet charge serves well for identifying the charge of the primordial parton of the hard scattering. In this Letter, we will apply the jet charge observable in the production of Higgs + 2 jets to discriminate between the Higgs production mechanisms at the LHC and to further constrain the Higgs couplings to gauge bosons.

Collider simulation.—We perform a detailed Monte Carlo simulation to explore the potential of the LHC for discriminating between Higgs production mechanisms and probing the hVV couplings via jet charge correlations. We generate both the W/Z fusion and GGF Higgs production processes at the 14 TeV LHC by MadGraph5 [61] at the parton level with the CT14LO parton distribution functions (PDFs) [62]. The following basic cuts for the jets are required in the partonic final state: $p_T^j > 20$ GeV with $|\eta_j| < 5$, where p_T^j and η_j denote the transverse momentum and rapidity of jet, respectively. The GGF process was generated under the heavy top quark limit, i.e., the effective field theory operator $\alpha_s/(12\pi v) h G^a_{\mu\nu} G^{\mu\nu,a}$, which provides a good approximation when the top quarks inside the loop are off shell. To get the isolated jets, we require the cone distance between the two jets $\Delta R > 0.4$. To suppress the contribution from the GGF process, we further require the invariant mass of jet pair $m_{jj} > 110$ GeV and rapidity gap between the two jets $|\Delta\eta_{jj}| > 2.5$. The jet is defined based on the anti-k_T algorithm [63] with the radius parameter $R = 0.4$. Then we pass the events to PYTHIA [64,65] for parton showering and hadronization. At the analysis level, all the events are required to pass a set of selection cuts following the settings from Ref. [19],

$$\begin{aligned} &p_T^j > 30 \text{ GeV}, \qquad 1 < |\eta_j| < 4.5, \\ &m_{jj} > 120 \text{ GeV}, \qquad |\Delta\eta_{jj}| > 3.5, \qquad |\eta_h| < 2.5, \end{aligned} \tag{3}$$

where η_h is the pseudorapidity of the Higgs boson.

On average the sign of the jet charge is consistent with the charge of the parton which evolves into the jet from the measurements at the LHC [58,59]. Therefore, the charge correlations for different VBF channels indicate the charge correlations of the parton in the hard process. Figure 2 shows the jet charge correlations between the leading and subleading jets from the W-fusion, Z-fusion, and GGF processes after the kinematic cuts [see Eq. (3)] with the benchmark jet charge parameter $\kappa = 0.3$. It clearly shows that the opposite sign of the two leading jet charges is favored in the W-fusion process due to the partonic nature of the hard scattering at the leading order. However, this feature disappears in the Z-fusion and GGF processes. It arises from the fact that both the opposite and same sign electric charges of the two leading jets in Z fusion could be generated with a comparable production rate, while the sign

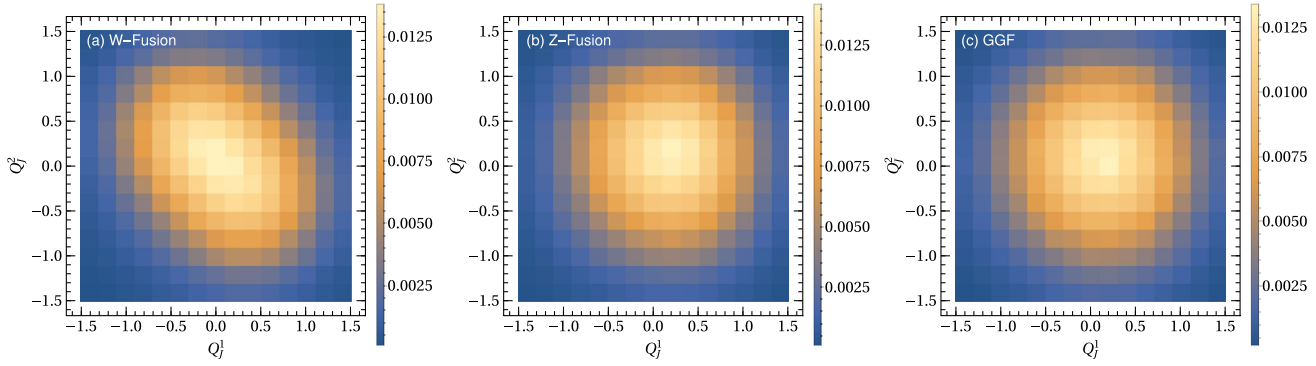

FIG. 2. The jet charge correlations between the leading and subleading jets from W-fusion, Z-fusion, and GGF processes with jet charge parameter $\kappa = 0.3$.

of the jet charges in the GGF process is arbitrary. Motivated by this, we define the jet charge asymmetry of the two leading jets in Higgs + 2 jets production by

$$A_Q = \left| \frac{Q_J^1 - Q_J^2}{Q_J^1 + Q_J^2} \right|, \tag{4}$$

where $Q_J^{1,2}$ is the jet charge of the leading and subleading jets, respectively. The advantage of this observable is that the systematic uncertainties, which are the dominant errors in jet charge measurements at the ATLAS and CMS Collaborations [58,59], are expected to be canceled. This conclusion has been verified by the previous studies of other track-based observables in the HERA measurement [66]. On the other hand, the jet charge distributions are sensitive only to the weight of the jet flavor of final states in the hard scattering but not to the Higgs decay information (i.e., the Higgs width and the other possible new physics effects in Higgs decay). However, the jet charge asymmetry in Eq. (4) may be unstable since it can be much enhanced for the events with $Q_J^1 + Q_J^2 \sim 0$; therefore, we will utilize the average values of the jet charges to define this asymmetry in this Letter, i.e.,

$$\bar{A}_Q \equiv \frac{\langle |Q_J^1 - Q_J^2| \rangle}{\langle |Q_J^1 + Q_J^2| \rangle} \equiv \frac{\langle Q^{(-)} \rangle}{\langle Q^{(+)} \rangle}, \tag{5}$$

where $\langle Q \rangle$ denotes the average value of the quantity Q and $Q^{(\pm)} = |Q_J^1 \pm Q_J^2|$. From the definition, if the charges have the opposite sign such as the partonic process for the W-fusion case, the asymmetry is expected to be $\bar{A}_Q > 1$. However, if the charges have the same sign, e.g., the Z-fusion process $uu \to uuh$, $\bar{A}_Q < 1$. For the GGF process the charges are fully uncorrelated so that $\bar{A}_Q \sim 1$.

Figure 3 shows the jet charge asymmetry $\bar{A}_Q$ as a function of the average transverse momentum of the two leading jets [$\bar{p}_T \equiv (p_T^1 + p_T^2)/2$] in Higgs + 2 jets production at the 14 TeV LHC with the integrated luminosity $\mathcal{L} = 300$ fb^{-1}. The statistical uncertainties are estimated from the PYTHIA simulation by generating a large number of pseudoexperiments. We assume that the statistical errors follow the Gaussian distribution and could be rescaled to any integrated luminosity by the event numbers. We have checked that $\bar{A}_Q$ does not noticeably depend on the choice of κ value, when varying from 0.3 to 0.7. As expected we find $\bar{A}_Q > 1$ for the W fusion (black points) since the sign of the jet charges is opposite. However, the asymmetry is close to 1 for the Z fusion as shown with blue points in Fig. 3. To further understand the behavior of the Z fusion, we also show $\bar{A}_Q$ for the Z fusion with opposite (red points) and same sign jet charges (cyan points) in the same figure, and the results are consistent with the argument before. When we combine all possible channels, this asymmetry would be close to 1 for the Z-fusion process since the opposite and same sign jet charge configurations could give a comparable contribution. The dominant contributions for the GGF process come from the qg and gg initial states; as a result, we could expect that $\bar{A}_Q \sim 1$ due to the uncorrelated nature of the jet charges in this process.

We also notice that the jet charge asymmetry is not very sensitive to $\bar{p}_T$ for the Z-fusion and the GGF processes.

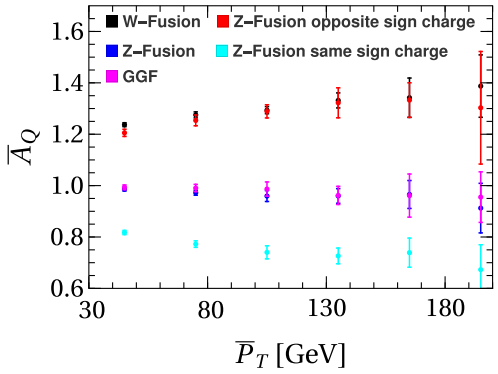

FIG. 3. The jet charge asymmetry $\bar{A}_Q$ distributions as a function of the average transverse momentum of the two leading jets $\bar{p}_T$ at the 14 TeV LHC with the integrated luminosity $\mathcal{L} = 300$ fb^{-1}. Its systematic uncertainties are assumed to cancel out.

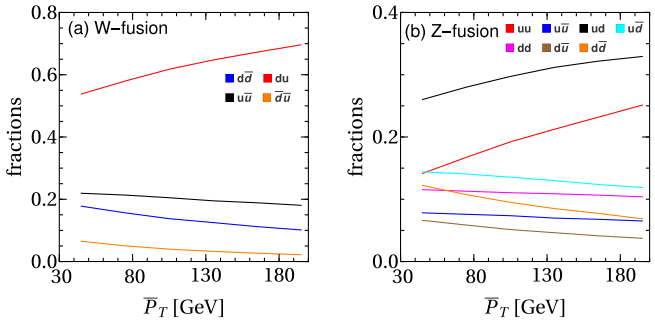

FIG. 4. Various initial state (qq') fraction distributions $f_{qq'}$ for Higgs + 2 jets production via W fusion and Z fusion at the 14 TeV LHC, as a function of the average jet $\bar{p}_T$.

In particular, it exhibits a weak $\bar{p}_T$ dependence for the W fusion and the Z fusion with opposite or same sign jet charges. To be clear about the $\bar{p}_T$ dependence for the W and the Z-fusion processes, we calculate various initial state (qq') fraction distributions $f_{qq'}$ for the W fusion and the Z fusion after the kinematic cuts in Eq. (3) at the leading order; see Fig. 4. It shows that the du quark initial state dominates the cross section in W fusion [see Fig. 4(a)], and it will induce a weak $\bar{p}_T$ dependence for the charge asymmetry in Fig. 3 (black points). For the Z-fusion process, we only show the fractions of the dominated channels in Fig. 4(b). The weak $\bar{p}_T$ dependence for the charge asymmetry of the Z fusion with opposite (red points in Fig. 3) and same sign (cyan points in Fig. 3) jet charges can also be understood from the behavior of the dominated fractions f_{ud} and f_{uu}. As a consequence, the jet charge asymmetry of the Z fusion will not be sensitive to the $\bar{p}_T$ after we combine all the subprocesses.

Next, we utilize the $\bar{A}_Q$ information to constrain the hVV couplings. After combing the W-fusion, Z-fusion, and GGF cross sections, the jet charge asymmetry in Higgs + 2 jets process reads as

$$\bar{A}_Q^{\rm tot} = \frac{f_W\langle Q^{(-)}\rangle_W + f_Z\langle Q^{(-)}\rangle_Z + f_G\langle Q^{(-)}\rangle_G}{f_W\langle Q^{(+)}\rangle_W + f_Z\langle Q^{(+)}\rangle_Z + f_G\langle Q^{(+)}\rangle_G}, \quad (6)$$

where the subscripts W, Z, and G represent the contribution from different channels accordingly. The fraction $f_i(\bar{p}_T, \kappa_{W/Z})$ is defined as $\sigma_i/(\sigma_W + \sigma_Z + \sigma_G)$ with $i = W$, Z, G. It shows that the W-boson fusion dominates the cross section after applying the kinematic cuts in Eq. (3). The contamination from GGF can be further suppressed with a boosted decision trees analysis, as shown in Fig. 2 of Ref. [67]. To estimate the impact of the jet charge asymmetry on constraining the hVV couplings, we consider $h \to WW^*(\to 2\ell 2\nu_\ell)$ and $ZZ^*(\to 4\ell)$, with $\ell = e, \mu, \tau$, as our benchmark decay processes in this work. The dominant background with these decay products is the GGF process [68]. But we emphasize that the correlations between κ_W and κ_Z measured from jet charges would not be sensitive to the Higgs decay information, which has been canceled in the definition of fractions. It can only change the statistical uncertainties in each $\bar{p}_T$ bin through the event numbers. The result could potentially be improved if we combine more decay modes of the Higgs boson, which is however beyond the scope of this work. Performing the pseudoexperiments, we conduct a combined χ^2 analysis as

$$\chi^2 = \sum_i \left[\frac{\bar{A}_Q^{i,\rm tot} - \bar{A}_Q^{i,\rm tot,0}}{\delta\bar{A}_Q^{i,\rm tot}}\right]^2, \quad (7)$$

where $\bar{A}_Q^{i,\rm tot,0}$ and $\delta\bar{A}_Q^{i,\rm tot}$ are the jet charge asymmetry in the SM (i.e., $\kappa_W = \kappa_Z = 1$) and the statistical uncertainty of the ith bin, respectively. For simplicity, we have assumed that the experimental values of the jet charges agree with the SM predictions. Note that we have rescaled the statistical uncertainties to include the branching ratio $\mathrm{BR}(h \to 2\ell 2\nu_\ell/4\ell)$ in each bin in our χ^2 analysis. The kinematic cuts for the decay products of the Higgs boson can also change the total event numbers. However, such effects should not significantly change the conclusions of this Letter and will be ignored in the following analysis. It shows that the typical error of $\bar{A}_Q^{\rm tot}$ is around $\mathcal{O}(1\%)$, which strongly depends on the average jet $\bar{p}_T$.

In Fig. 5, we show the expected limits on the hVV couplings at the 68% confidence level (C.L.) for the integrated luminosity 3000 fb^{-1}, obtained from the jet charge asymmetries (red band) at the 14 TeV LHC (HL LHC). It is evident that κ_W and κ_Z cannot be uniquely determined by the measurement of jet charge asymmetry alone. In order to further reduce the error band in the parameter space of κ_W and κ_Z, without making any

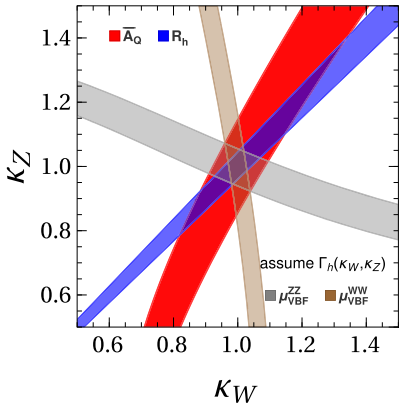

FIG. 5. The expected constraints at the HL LHC on $\kappa_{W,Z}$ from the jet charge asymmetry $\bar{A}_Q$ (red). The blue region is bounded by the R_h in $gg \to h$ production. The gray and brown regions represent the constraints from the VBF Higgs signal strength measurements via the decay modes $h \to ZZ^*$ and $h \to WW^*$, respectively, and they depend on the assumption of the Higgs boson width Γ_h.

assumption on the total decay width (Γ_h) of the Higgs boson, we consider the following ratio of the Higgs signal strength measurements:

$$R_h \equiv \frac{\mu(gg \to h \to WW^*)}{\mu(gg \to h \to ZZ^*)} = \frac{\kappa_W^2}{\kappa_Z^2}, \tag{8}$$

where the signal strength modifier $\mu(gg \to h \to VV^*)$ is defined as the measured cross section relative to the SM expectation. Hence, any new physics contributions to the $gg \to h$ production cross section would cancel in R_h. Its constraint on κ_W and κ_Z at the HL LHC is shown as the blue band in Fig. 5, where the error of R_h is taken to be 5.7% [69]. It is evident that the combined analysis of the $\bar{A}_Q^{\rm tot}$ and R_h data can further constrain the allowed κ_W and κ_Z values at the HL LHC. We note that the correlation between κ_W and κ_Z, extracted from $\bar{A}_Q^{\rm tot}$, is dependent of the fraction ($f_{W,Z}$) of production cross section contributed by various subprocesses, which is sensitive to the kinematic selection of the VBF events. Hence, it is possible to apply some advanced technologies, such as boosted decision tree or machine learning, to further improve the constraints on κ_W and κ_Z, which is however beyond the scope of this work.

For completeness, we also show in Fig. 5 the expected limits from the Higgs signal strength measurements of the VBF Higgs production with $h \to WW^*$ (denoted by $\mu_{\rm VBF}^{WW}$ in the figure, brown region) and $h \to ZZ^*$ (denoted by $\mu_{\rm VBF}^{ZZ}$ in the figure, gray region) at the HL LHC [69]. Here, the error of the signal strength of the VBF production with $h \to WW^*$ and $h \to ZZ^*$ is taken to be 5.5% and 9.5%, respectively [69]. We note that while the constraints imposed by the $\bar{A}_Q^{\rm tot}$ and R_h data are independent of Γ_h, those imposed by $\mu_{\rm VBF}^{WW}$ and $\mu_{\rm VBF}^{ZZ}$ are dependent of the assumption made in the calculation of Γ_h. Here, we assumed that Γ_h is only modified by the values of κ_W and κ_Z.

Conclusions.—In this Letter, we propose a novel and feasible method to separate the W-fusion from the Z-fusion and the GGF processes by utilizing the jet charge asymmetry $\bar{A}_Q$ of the two leading jets in Higgs + 2 jets production at the HL LHC. This is crucial for determining the couplings of the Higgs boson to W^+W^- and ZZ gauge bosons, without the need of making any assumption about the decay width of the Higgs boson. Owing to the partonic nature of the hard scattering, we demonstrate that the asymmetry $\bar{A}_Q > 1$ for W fusion, while it is always close to 1 for the Z-fusion and the GGF processes. Such a different feature can be used to discriminate between the Higgs production mechanisms and to determine the Higgs couplings to the gauge bosons κ_V. While the usual methods of determining κ_V from the Higgs signal strength measurement depends on the assumption of Γ_h, the proposed measurement of $\bar{A}_Q^{\rm tot}$ does not rely on such an assumption.

H. T. L. is supported by the National Science Foundation of China under Grant No. 12275156. B. Y. is supported by the IHEP under Contract No. E25153U1. C. P. Y. is supported by the U.S. National Science Foundation under Grant No. PHY-2013791 and is grateful for the support from the Wu-Ki Tung endowed chair in particle physics.

*haitao.li@sdu.edu.cn
†Corresponding author.
yanbin@ihep.ac.cn
‡yuan@pa.msu.edu

[1] C. Englert, A. Freitas, M. M. Mühlleitner, T. Plehn, M. Rauch, M. Spira, and K. Walz, J. Phys. G **41**, 113001 (2014).
[2] K. Cheung, J. S. Lee, and P.-Y. Tseng, Phys. Rev. D **90**, 095009 (2014).
[3] J. Bergstrom and S. Riad, Phys. Rev. D **91**, 075008 (2015).
[4] A. Falkowski, Pramana **87**, 39 (2016).
[5] N. Craig, J. Gu, Z. Liu, and K. Wang, J. High Energy Phys. 03 (2016) 050.
[6] T. Corbett, O. J. P. Eboli, D. Goncalves, J. Gonzalez-Fraile, T. Plehn, and M. Rauch, J. High Energy Phys. 08 (2015) 156.
[7] G. Durieux, C. Grojean, J. Gu, and K. Wang, J. High Energy Phys. 09 (2017) 014.
[8] J. De Blas, G. Durieux, C. Grojean, J. Gu, and A. Paul, J. High Energy Phys. 12 (2019) 117.
[9] Q.-H. Cao, L.-X. Xu, B. Yan, and S.-H. Zhu, Phys. Lett. B **789**, 233 (2019).
[10] C.-W. Chiang, X.-G. He, and G. Li, J. High Energy Phys. 08 (2018) 126.
[11] J. Ellis, M. Madigan, K. Mimasu, V. Sanz, and T. You, J. High Energy Phys. 04 (2021) 279.
[12] J. Y. Araz, S. Banerjee, R. S. Gupta, and M. Spannowsky, J. High Energy Phys. 04 (2021) 125.
[13] B. Yan, Phys. Lett. B **822**, 136709 (2021).
[14] K.-P. Xie and B. Yan, Phys. Lett. B **820**, 136515 (2021).
[15] W. Bizoń, F. Caola, K. Melnikov, and R. Röntsch, Phys. Rev. D **105**, 014023 (2022).
[16] S. Banerjee, R. S. Gupta, O. Ochoa-Valeriano, and M. Spannowsky, J. High Energy Phys. 02 (2022) 176.
[17] P. Sharma and A. Shivaji, J. High Energy Phys. 10 (2022) 108.
[18] K. Asteriadis, F. Caola, K. Melnikov, and R. Röntsch, Phys. Rev. D **107**, 034034 (2023).
[19] ATLAS Collaboration, Nature (London) **607**, 52 (2022).
[20] CMS Collaboration, Nature (London) **607**, 60 (2022).
[21] F. Caola and K. Melnikov, Phys. Rev. D **88**, 054024 (2013).
[22] J. M. Campbell, R. K. Ellis, and C. Williams, Phys. Rev. D **89**, 053011 (2014).
[23] J. S. Gainer, J. Lykken, K. T. Matchev, S. Mrenna, and M. Park, Phys. Rev. D **91**, 035011 (2015).
[24] C. S. Li, H. T. Li, D. Y. Shao, and J. Wang, J. High Energy Phys. 08 (2015) 065.
[25] A. M. Sirunyan *et al.* (CMS Collaboration), Phys. Rev. D **99**, 112003 (2019).
[26] A. Tumasyan *et al.* (CMS Collaboration), Nat. Phys. **18**, 1329 (2022).

[27] C. Englert and M. Spannowsky, Phys. Rev. D **90**, 053003 (2014).
[28] G. Cacciapaglia, A. Deandrea, G. D. La Rochelle, and J.-B. Flament, Phys. Rev. Lett. **113**, 201802 (2014).
[29] C. Englert, Y. Soreq, and M. Spannowsky, J. High Energy Phys. 05 (2015) 145.
[30] S. J. Lee, M. Park, and Z. Qian, Phys. Rev. D **100**, 011702(R) (2019).
[31] Q.-H. Cao, B. Yan, C. P. Yuan, and Y. Zhang, Phys. Rev. D **102**, 055010 (2020).
[32] A. Azatov *et al.*, Report No. LHCHWG-2022-001, 2022.
[33] V. D. Barger, K.-m. Cheung, T. Han, J. Ohnemus, and D. Zeppenfeld, Phys. Rev. D **44**, 1426 (1991).
[34] V. D. Barger, K.-m. Cheung, T. Han, and D. Zeppenfeld, Phys. Rev. D **44**, 2701 (1991); **48**, 5444(E) (1993).
[35] N. Kauer, T. Plehn, D. L. Rainwater, and D. Zeppenfeld, Phys. Lett. B **503**, 113 (2001).
[36] V. Rentala, N. Vignaroli, H.-n. Li, Z. Li, and C. P. Yuan, Phys. Rev. D **88**, 073007 (2013).
[37] P. Sun, C. P. Yuan, and F. Yuan, Phys. Lett. B **762**, 47 (2016).
[38] C.-H. Chan, K. Cheung, Y.-L. Chung, and P.-H. Hsu, Phys. Rev. D **96**, 096009 (2017).
[39] T. Liu, K. Melnikov, and A. A. Penin, Phys. Rev. Lett. **123**, 122002 (2019).
[40] P. Sun, C. P. Yuan, and F. Yuan, Phys. Lett. B **797**, 134852 (2019).
[41] C.-W. Chiang, D. Shih, and S.-F. Wei, Phys. Rev. D **107**, 016014 (2023).
[42] R. D. Field and R. P. Feynman, Nucl. Phys. **B136**, 1 (1978).
[43] D. Krohn, M. D. Schwartz, T. Lin, and W. J. Waalewijn, Phys. Rev. Lett. **110**, 212001 (2013).
[44] W. J. Waalewijn, Phys. Rev. D **86**, 094030 (2012).
[45] K. Fraser and M. D. Schwartz, J. High Energy Phys. 10 (2018) 093.
[46] A. J. Larkoski and E. M. Metodiev, J. High Energy Phys. 10 (2019) 014.
[47] A. Gianelle, P. Koppenburg, D. Lucchesi, D. Nicotra, E. Rodrigues, L. Sestini, J. de Vries, and D. Zuliani, J. High Energy Phys. 08 (2022) 014.
[48] Y. C. J. Chen, C.-W. Chiang, G. Cottin, and D. Shih, Phys. Rev. D **101**, 053001 (2020).
[49] H. T. Li, B. Yan, and C. P. Yuan, Phys. Lett. B **833**, 137300 (2022).
[50] X. Wong and B. Yan, arXiv:2302.02084.
[51] S.-Y. Chen, B.-W. Zhang, and E.-K. Wang, Chin. Phys. C **44**, 024103 (2020).
[52] H. T. Li and I. Vitev, Phys. Rev. D **101**, 076020 (2020).
[53] H. T. Li and I. Vitev, Phys. Rev. Lett. **126**, 252001 (2021).
[54] Z.-B. Kang, X. Liu, S. Mantry, and D. Y. Shao, Phys. Rev. Lett. **125**, 242003 (2020).
[55] Z.-B. Kang, X. Liu, S. Mantry, M. C. Spraker, and T. Wilson, Phys. Rev. D **103**, 074028 (2021).
[56] K. Lee, J. Mulligan, M. Płoskoń, F. Ringer, and F. Yuan, J. High Energy Phys. 03 (2023) 085.
[57] V. Khachatryan *et al.* (CMS Collaboration), J. High Energy Phys. 12 (2014) 017.
[58] G. Aad *et al.* (ATLAS Collaboration), Phys. Rev. D **93**, 052003 (2016).
[59] A. M. Sirunyan *et al.* (CMS Collaboration), J. High Energy Phys. 10 (2017) 131.
[60] A. M. Sirunyan *et al.* (CMS Collaboration), J. High Energy Phys. 07 (2020) 115.
[61] J. Alwall, R. Frederix, S. Frixione, V. Hirschi, F. Maltoni, O. Mattelaer, H. S. Shao, T. Stelzer, P. Torrielli, and M. Zaro, J. High Energy Phys. 07 (2014) 079.
[62] S. Dulat, T.-J. Hou, J. Gao, M. Guzzi, J. Huston, P. Nadolsky, J. Pumplin, C. Schmidt, D. Stump, and C. P. Yuan, Phys. Rev. D **93**, 033006 (2016).
[63] M. Cacciari, G. P. Salam, and G. Soyez, J. High Energy Phys. 04 (2008) 063.
[64] T. Sjöstrand, S. Ask, J. R. Christiansen, R. Corke, N. Desai, P. Ilten, S. Mrenna, S. Prestel, C. O. Rasmussen, and P. Z. Skands, Comput. Phys. Commun. **191**, 159 (2015).
[65] C. Bierlich *et al.*, SciPost Phys. Codebases 8 (2022).
[66] F. D. Aaron *et al.* (H1 Collaboration), Phys. Lett. B **681**, 125 (2009).
[67] ATLAS Collaboration, arXiv:2208.02338.
[68] ATLAS Collaboration, Technical Report, CERN, Geneva, 2016, https://cds.cern.ch/record/2145377.
[69] M. Cepeda *et al.*, CERN Yellow Rep. Monogr. **7**, 221 (2019).